

NMR Spectroscopy

Deutsche Ausgabe: DOI: 10.1002/ange.201603205
Internationale Ausgabe: DOI: 10.1002/anie.201603205 Selective Protein Hyperpolarization in Cell Lysates Using Targeted Dynamic Nuclear Polarization

Thibault Viennet, Aldino Viegas, Arne Kuepper, Sabine Arens, Vladimir Gelev, Ognyan Petrov, Tom N. Grossmann, Henrike Heise, and Manuel Etzkorn*

Abstract: Nuclear magnetic resonance (NMR) spectroscopy has the intrinsic capabilities to investigate proteins in native environments. In general, however, NMR relies on non-natural protein purity and concentration to increase the desired signal over the background. We here report on the efficient and specific hyperpolarization of low amounts of a target protein in a large isotope-labeled background by combining dynamic nuclear polarization (DNP) and the selectivity of protein interactions. Using a biradical-labeled ligand, we were able to direct the hyperpolarization to the protein of interest, maintaining comparable signal enhancement with about 400-fold less radicals than conventionally used. We could selectively filter out our target protein directly from crude cell lysate obtained from only 8 mL of fully isotope-enriched cell culture. Our approach offers effective means to study proteins with atomic resolution in increasingly native concentrations and environments.

Structural biology is gradually recognizing the indispensable link between the properties of the target protein and its native environment. Nuclear Magnetic Resonance (NMR) spectroscopy has contributed to this notion by for example, enabling measurements in cells,^[1] cell envelopes^[2] or cellular milieus.^[3] The increasing complexity of such environments is however accompanied by two main challenges: (i) large contribution of unwanted background signals and (ii) low sensitivity of the

target protein. Therefore, cellular NMR approaches so far rely on selective isotope-labeling strategies that favor the target protein over the background, for example, by changing the medium before protein overexpression^[2] or (re)introducing the purified isotope-labeled protein into an unlabeled environment.^[1,3] Dynamic nuclear polarization (DNP), that is, the enhancement of the NMR signal due to transfer of the high polarization of a free electron to the nuclei, has the potential to overcome sensitivity limitations associated with low protein concentrations.^[4] DNP relies, in general, on an empirically optimized statistical distribution of (bi)radicals in the sample,^[5] and has been successfully applied to study challenging biological systems.^[2,3,6] Additionally, the concept of placing the radical in a more defined position has recently emerged, for example, attached to a nanocrystalline peptide,^[7] endogenously paramagnetic interaction partners or proteins,^[8] lipid-anchored radicals^[9] and radicals directly attached to membrane proteins.^[10] In line with these localized DNP techniques, we here report on a broadly applicable approach to selectively excite a target protein over a large background. Basis of this targeted DNP approach is the covalent attachment of the biradical TOTAPOL^[5b] to an interaction partner of the target protein. The selectivity of the protein interaction is then exploited to specifically direct the hyperpolarization to the protein of interest. Using the 20 kDa protein Bcl-x_L (target) and its binding partner, the Bak peptide (ligand), we show that comparable protein signal enhancements can be achieved with several hundred fold less radicals than conventionally used, largely confining the hyperpolarization to the targeted protein instead of the whole sample. We demonstrate the potential of the setup by selectively hyperpolarizing our target protein directly in its crude, fully isotope-enriched cell lysate. Notably, except for the standard protein overexpression, our DNP data were obtained without increasing the protein levels (concentration or purity) as compared to the living cells.

To generate the radical-labeled ligand, we introduce a simple one-step synthesis of maleimide modified TOTAPOL (mTP) which allows the covalent attachment to cysteine side chains (Figure 1a). Purified mTP was then ligated to a derivative of the Bak peptide containing an N-terminal cysteine connected by a PEG linker to a 16-residue Bak fragment which is known to interact with Bcl-x_L^[11] (Figure 1b, also see the Methods section and Figures S1–3 in the Supporting Information). Binding of the modified Bak peptide can be detected by chemical shift perturbations in solution NMR spectra. Analysis of the peak volumes of bound and free Bcl-x_L shows that around 90% of Bcl-x_L is bound to modified Bak (Figure 1d, molar ratio 1:1). This fits

[*] T. Viennet, Dr. A. Viegas, S. Arens, Prof. Dr. H. Heise, Dr. M. Etzkorn
Institute of Physical Biology
Heinrich Heine University
Universitätsstr. 1, 40225 Düsseldorf (Germany)
and

Institute of Complex Systems (ICS-6)

Forschungszentrum Jülich

Wilhelm Jönin Strasse, Jülich (Germany)

E-mail: manuel.etzkorn@hhu.de

A. Kuepper, Prof. Dr. T. N. Grossmann

Chemical Genomics Centre of the Max Planck Society

Otto-Hahn-Str. 15, 44227 Dortmund (Germany)

Prof. Dr. T. N. Grossmann

VU University Amsterdam

Department of Chemistry and Pharmaceutical Sciences

De Boelelaan 1083


1081 HV Amsterdam (The Netherlands)

Prof. Dr. V. Gelev, Prof. Dr. O. Petrov

Faculty of Chemistry and Pharmacy

Sofia University

1 James Bourchier Blvd., 1164 Sofia (Bulgaria)

 Supporting information and the ORCID identification number(s) for the author(s) of this article can be found under <http://dx.doi.org/10.1002/anie.201603205>.

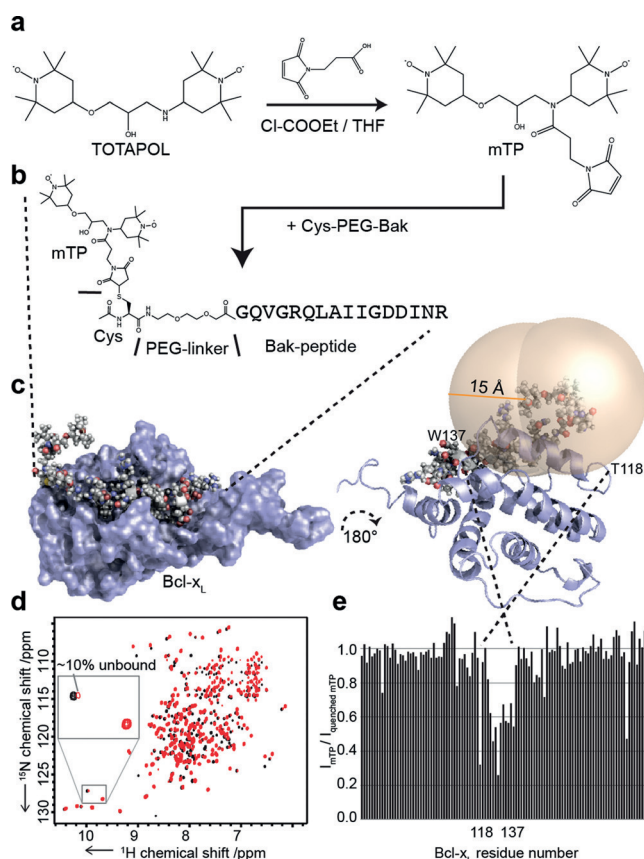


Figure 1. Preparation of radical-labeled ligand (Bak-mTP) and characterization of its interaction with the target protein (Bcl-x_L). a) One-step reaction for mTP synthesis. b) Ligand design (see the Supporting Information for more details). c) Structural model of the complex between Bak-mTP and Bcl-x_L.^[11] d) Comparison of ^{15}N - ^1H -HSQC spectra of free Bcl-x_L (black) vs. complex (red, 1:1 molar). e) PRE plot as the ratio of peak volumes in oxidized vs. reduced radical states for all resolved Bcl-x_L residues. A well-defined protein region is affected by the biradical (in line with the radical localization shown in c).

well the expected ratio of 91.2%, based on a K_D of 340 nM found for the unmodified Bak peptide.^[11] We also performed Paramagnetic Relaxation Enhancement (PRE) measurements that identified only one well-defined region of Bcl-x_L affected by the presence of the biradical (Figure 1e, Figure S4). Overall the solution NMR data could confirm binding of the modified ligand, report on at least a partial integrity of the unpaired electron spin and allow for an initial estimation of the location of the radicals in our system.

We subsequently tested our setup under DNP conditions (Figure 2). All DNP spectra were recorded at 600 MHz proton resonance frequency at 108 K. Initially we recorded reference spectra under conventional DNP conditions using 20 mM soluble TOTAPOL and 23 μg of uniformly ^{13}C -, ^{15}N -labeled Bcl-x_L in standard buffer conditions^[12] (50% [D₈]glycerol, 10% [D₆]DMSO, 30% D₂O, and 10% H₂O). Note that this buffer only slightly differs from the optimal “DNP-juice” by replacing 10% of the glycerol with DMSO to ensure solubility of the ligand. Using these conditions, an enhancement factor ϵ (ratio of signal-to-noise in the presence and absence of microwaves) of 20 was obtained (Figure 2a).

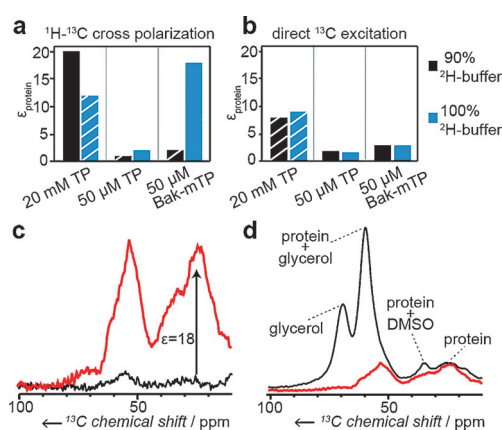


Figure 2. Targeted DNP provides effective and selective hyperpolarization. a) DNP enhancements of ^1H - ^{13}C cross polarization for Bcl-x_L in the presence of indicated amounts of soluble TOTAPOL (TP) or in the Bak-mTP targeted setup. All experiments were recorded using 23 μg of purified Bcl-x_L and either conventional 10% protonation (black) or fully deuterated buffers (blue). Stripe pattern indicate values that were determined with less accuracy (see Figure S6 for all experimental data). b) Same samples as in a) but using direct ^{13}C excitation. c) ^1H - ^{13}C cross polarization spectra of the optimized targeted DNP setup in the presence (red) and absence (black) of microwave irradiation. d) Comparison of targeted (red) and best conventional (black) setup showing a strongly protein-directed hyperpolarization in the targeted setup.

Placing the radical in a well-defined (close) distance should allow the usage of only one biradical per target protein. Using a protein concentration of about 50 μM will then reduce the free radical concentration 400-fold as compared to the conventional setup. To test the DNP properties of these low radical concentrations we recorded reference spectra of 50 μM Bcl-x_L in the presence of 50 μM free TOTAPOL. As expected, this low radical concentration does not sufficiently hyperpolarize the sample (ϵ around 1). Surprisingly, we experienced also weak enhancement factors ($\epsilon = 2$) when using the targeted setup under standard buffer protonation level (10%). We attribute this to spin diffusion effects that may pull the polarization away from the protein and into the buffer.^[13] Indeed, when changing to a fully deuterated buffer the enhancement factor of the targeted setup is drastically increased leading to a value of $\epsilon = 18$. Note that this should translate to a value between 27 and 40 at 400 MHz^[14] for which most previous values are reported.

The hypothesis of ^1H -polarization leakage into the protonated buffer is supported by the enhancement factors of direct carbon excitation, which are not affected by buffer protonation levels (Figure 2b). Noteworthy, the rather low enhancement of the ^{13}C nuclei in the targeted setup may indicate that the distance between the biradical and the ^{13}C -enriched protein is too long for an effective hyperpolarization and hence may contribute to the fundamental understanding of the effective enhancement radius of the biradical. On the proton side, we detect an increase in the DNP-build up time τ_{DNP} for the covalently bound biradical (Figure S5) and see a strong effect of the buffer protonation level but we do not experience a far-reaching quenching and/or depolarization effect (Figure S5). The herein observed significantly higher

enhancement factor, as compared to most previous localized DNP studies, is likely directly related to the latter findings and may be attributed to the low total amount of radicals used in our setup.

A comparison of the conventional and targeted 1D DNP spectra demonstrates the selectivity of the targeted setup (Figure 2d). While the protein-specific signal (peak at 25 ppm) has a similar magnitude, the background-specific peak (at 75 ppm) is largely reduced in the targeted setup (also see Figure S7). All in all, the initial DNP characterization of our targeted setup reveals that (i) one biradical provides hyperpolarization in the target protein with an enhancement factor similar to that of a proton network polarized with 400-fold more radicals, (ii) the quenching/depolarization effects of the mTP are rather moderate and (iii) the directed hyperpolarization drastically improves the protein-over-background signal. Because of the large effects of buffer protonation, all further targeted experiments were carried out in fully deuterated buffer. Note that while the herein used buffer condition was chosen to allow a fair comparison between conventional and targeted DNP, it in general deviates from the native cellular environment. It has been shown before that localized DNP setups, however, can extend the range of suitable DNP buffer conditions and, depending on the biological system and scientific question, an alternative buffer may be selected to reduce potential artifacts from non-native buffer conditions.^[10b]

To test our targeted approach in an isotope-labeled background, we used samples of Bcl-x_L with 100-fold molar excess of isotope-labeled glycine. Due to the good separation of glycine C α signals from other aliphatic carbons, the C α -CO cross peaks in the 2D PDSD spectrum provide an estimate of the labeled background over Bcl-x_L signal. While in the conventional setup the glycine signal largely exceeds the protein specific signals (Figure 3a,d, red), it is significantly reduced (by around 80%) in the targeted setup (Figure 3b,e, red; Figure S8).

Theoretically, this selective enhancement should allow to obtain a pure spectrum of the target protein by subtracting a non-selective spectrum scaled to the same background level. Note that the quality of the difference spectrum will predominantly depend on the selective enhancement factor (see Figure S9). The non-selective spectrum could be a DNP-off spectrum or a DNP-on spectrum in a conventional setup. While the first could be obtained using only one sample, it may be limited by insufficient signal intensity. Here we subtracted the signal of the conventional DNP-on sample scaled to match the same glycerol intensity (Figure 3c,f, red). For this approach the protein to glycerol ratio needs to be identical in both samples, which can easily be achieved by splitting the same stock solutions. Indeed, the resulting difference spectrum does not show any apparent signals indicative of the glycine background anymore. This alludes that the targeted setup has the potential to selectively hyperpolarize one in a hundred molecules, enabling the investigation of small amounts of target protein in large, fully isotope-labeled backgrounds.

We subsequently applied our approach to study Bcl-x_L directly in its cell lysate using only one buffer exchange step

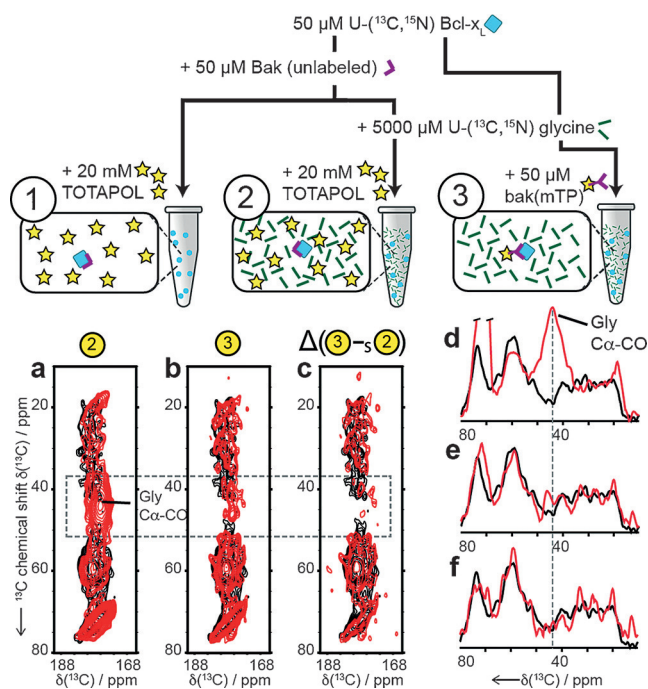


Figure 3. Targeted DNP can selectively enhance a protein over a large isotope labeled background. A schematic of the used samples (top) and overlay of the CO-Cx region of ¹³C, ¹³C-PDSD spectra of pure Bcl-x_L (black, sample 1) with data obtained in the presence of 100-fold molar excess of labeled glycine using conventional DNP (a, red, sample 2), targeted DNP (b, red, sample 3) and c) difference between the targeted and conventional DNP spectra (scaled to the same glycerol intensity). 1D projections of the 2D spectra in (a–c) onto the indirect dimension are shown in (d–f), respectively, and visualize the decrease of the glycine background.

and no protein purification. To challenge our approach, cell growth and protein expression were carried out in the same medium, leading to the same degree of labeling of background and target protein. Each DNP sample was prepared using only 8 mL of cell culture for which we estimate that the respective cell volume reflects the volume of the sample rotor (see the Supporting Information for calculation) resulting in samples with protein levels similar to the living cell. Four different samples were prepared including lysates in a targeted (sample I) and a conventional setup (sample II), as well as a positive (sample III) and a negative control (sample IV; Figure 4a). 1D spectra of the targeted and conventional samples are shown in Figure 4b. Due to the homogeneous hyperpolarization in the conventional setup the contribution of Bcl-x_L to the total signal should be given by its abundance, which we estimate based on our biochemical data to be about 10% of the total protein content. Scaling the obtained spectra to the same background signal (glycerol) reveals a protein-specific enhancement in the targeted setup (Figure 4c).

Interestingly, the Bcl-x_L protein differs from the average protein in the lysate due to an exceptionally high content in α -helical secondary structure. Since ¹³C chemical shifts are indicative of secondary structure^[15] we used a projection of the C α -CO cross-peaks to assess the secondary structure content of the spectra.^[3] While a comparison of the experimental data of purified Bcl-x_L to the predicted pure

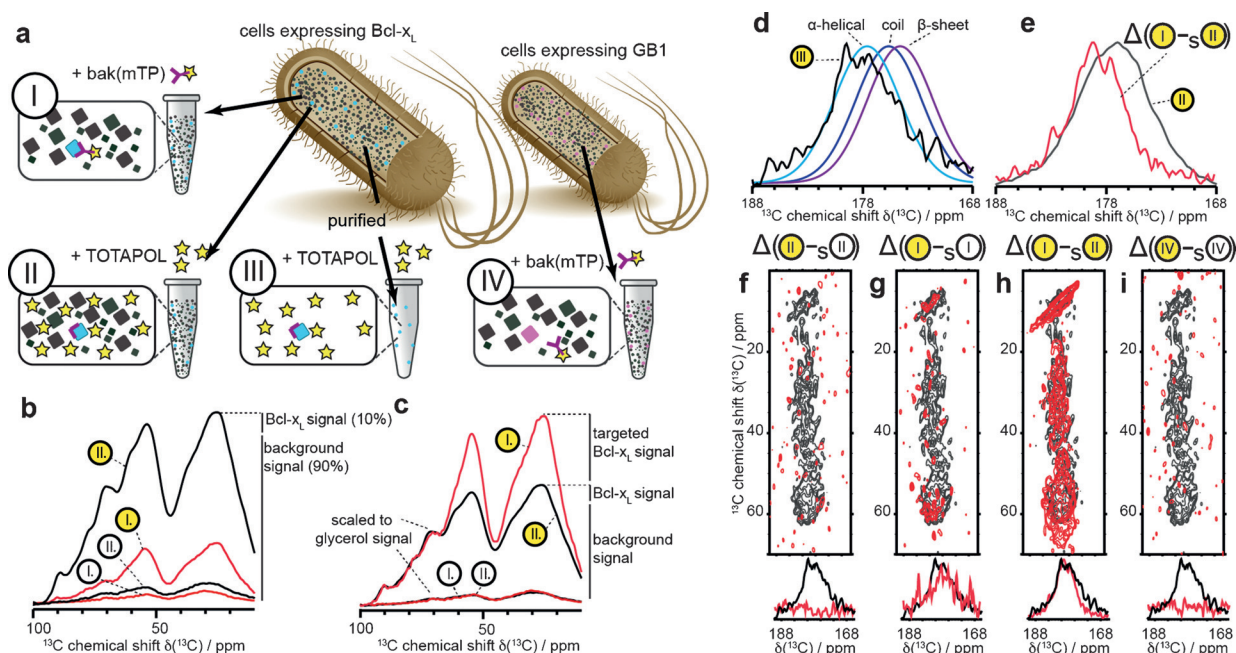


Figure 4. Targeted DNP is applicable to proteins at low abundance in crude cell lysates. a) Schematic of used samples. b) 1D spectra in the presence (yellow label) and absence (white label) of microwaves for the conventional (black) and targeted (red) setup. Expected signal contributions are indicated. c) Same spectra as in (b), but scaled to the glycerol background. d) Predicted CO signals for indicated secondary structure elements overlaid with a C α -CO projection of a 2D PDSD spectrum of purified Bcl-x_L (sample III). e) Comparison of the projections obtained from conventional DNP (sample II) and its difference to the targeted approach (sample I). A clear shift towards α -helical structure is visible. f–i) Comparison of indicated difference spectra (red) to the purified Bcl-x_L reference (sample III, gray) and corresponding C α -CO projections. Note that in all cases (f–i) a non-selective spectrum of the lysate was subtracted suggesting that residual signal, which is only found in the targeted DNP approach and only in the presence of Bcl-x_L (g,h), originated from a selective protein polarization.

secondary structure elements^[15] reflects the high α -helical content of the protein (Figure 4d), the conventional DNP spectrum of the cell lysate (Figure 4e, black) shows a considerable contribution of all secondary structure elements as expected for a heterogeneous cell lysate. Noteworthy, the signal difference between the targeted and the conventional DNP spectrum (after scaling to the same glycerol level) has a clear increase in α -helical content (Figure 4e, red), consistent with selectively filtering out the Bcl-x_L signal from the background.

To further validate the selectivity of the setup, a series of 2D PDSD difference spectra were measured (Figure 4f–i, red) and compared to the spectrum of purified Bcl-x_L (Figure 4f–i, black). As expected the difference of a conventional DNP-on and DNP-off spectrum (Figure 4f, red), results in an empty spectrum. The respective difference in the targeted setup (Figure 4g, red) contains a weak signal in the C α -CO region (also see projection). Here, the relative low signal-to-noise ratio is related to the weak signal of the DNP-off spectrum. Instead of recording a very long DNP-off spectrum, we subtracted a conventional DNP-on 2D PDSD spectrum of the same lysate preparation (scaled to the same glycerol signal). The resulting difference spectrum has a higher signal-to-noise ratio and nicely overlaps with the reference Bcl-x_L spectrum (Figure 4h). To further corroborate this observation, we designed a negative control with cell lysate grown under the same conditions but expressing a GB1-protein construct instead of Bcl-x_L. The difference

spectrum of the lysate containing GB1 using the same amount of Bak-mTP as before does not show any signal, confirming that this cell lysate does not specifically interact with the radical-labeled Bak peptide (Figure 4i).

In summary the lysate data indicate that (i) the targeted DNP setup specifically enhances protein signal over glycerol signal (Figure 4c), (ii) the additionally enhanced protein signal is predominantly α -helical (Figure 4e), (iii) the signal also largely overlaps with the signal of purified Bcl-x_L (Figure 4h) and (iv) subtracting an unspecific spectrum of the lysate results in a non-empty spectrum only for the targeted DNP-enhanced spectrum and only in the presence of the target protein (Figure 4f–i, Figures S10,S11). These data strongly suggest that the signal seen in Figure 4g,h originated from a specific interaction of Bak and Bcl-x_L.

Due to the power of DNP we could obtain spectra from only 8 mL of non-purified cell culture. In addition to a large reduction of workload and sample losses, the low amount of required isotopes will also facilitate usage of expensive labeling strategies. While the herein used target protein primarily serves as a suitable test system and will in general also be accessible to in-cell solution NMR approaches, we anticipate that future applications of the targeted DNP setup may also involve systems that are not soluble, cannot be easily purified, reintroduced into a cellular context, and/or require expensive isotope-labeled media, such as membrane proteins and/or eukaryotic expression systems. When combined with established selective and protein-over-background isotope-

labeling techniques, the targeted DNP setup may help to specifically visualize the target protein in front of a massive background and for example, probe the effects of molecular crowding, the native membrane environment and interactions with other cellular components on a residue specific level.

Acknowledgements

The authors acknowledge access to the Jülich-Düsseldorf Biomolecular NMR Center and funding through a Major Equipment Initiative (HE3243/4-1), two Emmy Noether grants of the DFG, grant number ET103/2-1 to M.E. and grant number GR3592/2-1 to T.N.G., a Marie Skłodowska-Curie Grant to A.V. (grant number 660258). We thank Dr. Dora Angelicheva from FB Reagents for assistance with flash chromatography. T.V. acknowledges support from the International NRW Research School iGRASP_{seed}. T.N.G. and A.K. were supported by AstraZeneca, Bayer CropScience, Bayer Health-Care, Boehringer Ingelheim, Merck KGaA, and the Max Planck Society.

Keywords: cell lysates · NMR spectroscopy · proteins · structure elucidation · structural biology

How to cite: *Angew. Chem. Int. Ed.* **2016**, *55*, 10746–10750
Angew. Chem. **2016**, *128*, 10904–10908

- [1] F. X. Theillet, A. Binolfi, B. Bekei, A. Martorana, H. M. Rose, M. Stuiver, S. Verzini, D. Lorenz, M. van Rossum, D. Goldfarb, P. Selenko, *Nature* **2016**, *530*, 45.
- [2] M. Kaplan, A. Cukkeman, G. C. van Zundert, S. Narasimhan, M. Daniels, D. Mance, G. Waksman, A. M. Bonvin, R. Fronzes, G. E. Folkers, M. Baldus, *Nat. Methods* **2015**, *12*, 649.
- [3] K. K. Frederick, V. K. Michaelis, B. Corzilius, T. C. Ong, A. C. Jacavone, R. G. Griffin, S. Lindquist, *Cell* **2015**, *163*, 620.
- [4] a) J. H. Ardenkjaer-Larsen, G. S. Boebinger, A. Comment, S. Duckett, A. S. Edison, F. Engelke, C. Griesinger, R. G. Griffin, C. Hilty, H. Maeda, G. Parigi, T. Prisner, E. Ravera, J. van Benthum, S. Vega, A. Webb, C. Luchinat, H. Schwalbe, L. Frydman, *Angew. Chem. Int. Ed.* **2015**, *54*, 9162; *Angew. Chem.* **2015**, *127*, 9292; b) U. Akbey, W. T. Franks, A. Linden, M. Orwick-Rydmark, S. Lange, H. Oschkinat, *Top. Curr. Chem.* **2013**, *338*, 181; c) Q. Z. Ni, E. Daviso, T. V. Can, E. Markhasin, S. K. Jawla, T. M. Swager, R. J. Temkin, J. Herzfeld, R. G. Griffin, *Acc. Chem. Res.* **2013**, *46*, 1933; d) E. J. Koers, E. A. van der Cruysen, M. Rosay, M. Weingarth, A. Prokofyev, C. Sauvee, O. Ouari, J. van der Zwan, O. Pongs, P. Tordo, W. E. Maas, M. Baldus, *J. Biomol. NMR* **2014**, *60*, 157.
- [5] a) D. A. Hall, *Science* **1997**, *276*, 930–932; b) C. Song, K. N. Hu, C. G. Joo, T. M. Swager, R. G. Griffin, *J. Am. Chem. Soc.* **2006**, *128*, 11385.
- [6] a) T. Jacso, W. T. Franks, H. Rose, U. Fink, J. Broecker, S. Keller, H. Oschkinat, B. Reif, *Angew. Chem. Int. Ed.* **2012**, *51*, 432; *Angew. Chem.* **2012**, *124*, 447; b) M. Renault, S. Pawsey, M. P. Bos, E. J. Koers, D. Nand, R. Tommassen-van Boxtel, M. Rosay, J. Tommassen, W. E. Maas, M. Baldus, *Angew. Chem. Int. Ed.* **2012**, *51*, 2998; *Angew. Chem.* **2012**, *124*, 3053; c) J. Maciejko, M. Mehler, J. Kaur, T. Lieblein, N. Morgner, O. Ouari, P. Tordo, J. Becker-Baldus, C. Glaubitz, *J. Am. Chem. Soc.* **2015**, *137*, 9032; d) M. L. Mak-Jurkauskas, V. S. Bajaj, M. K. Hornstein, M. Belenky, R. G. Griffin, J. Herzfeld, *Proc. Natl. Acad. Sci. USA* **2008**, *105*, 883.
- [7] V. Vitzthum, F. Borcard, S. Jannin, M. Morin, P. Mievil, M. A. Caporini, A. Sienkiewicz, S. Gerber-Lemaire, G. Bodenhausen, *ChemPhysChem* **2011**, *12*, 2929.
- [8] a) T. Maly, D. Cui, R. G. Griffin, A. F. Miller, *J. Phys. Chem. B* **2012**, *116*, 7055; b) P. Wenk, M. Kaushik, D. Richter, M. Vogel, B. Suess, B. Corzilius, *J. Biomol. NMR* **2015**, *63*, 97.
- [9] a) C. Fernandez-de-Alba, H. Takahashi, A. Richard, Y. Chenavier, L. Dubois, V. Maurel, D. Lee, S. Hediger, G. De Paepe, *Chem. Eur. J.* **2015**, *21*, 4512; b) A. N. Smith, M. A. Caporini, G. E. Fanucci, J. R. Long, *Angew. Chem. Int. Ed.* **2015**, *54*, 1542; *Angew. Chem.* **2015**, *127*, 1562.
- [10] a) E. A. van der Cruysen, E. J. Koers, C. Sauvee, R. E. Hulse, M. Weingarth, O. Ouari, E. Perozo, P. Tordo, M. Baldus, *Chem. Eur. J.* **2015**, *21*, 12971; b) M. A. Voinov, D. B. Good, M. E. Ward, S. Milikisiyants, A. Marek, M. A. Caporini, M. Rosay, R. A. Munro, M. Ljumovic, L. S. Brown, V. Ladizhansky, A. I. Smirnov, *J. Phys. Chem. B* **2015**, *119*, 10180; c) B. J. Wylie, B. G. Dzиковski, S. Pawsey, M. Caporini, M. Rosay, J. H. Freed, A. E. McDermott, *J. Biomol. NMR* **2015**, *61*, 361.
- [11] M. Sattler, H. Liang, D. Nettlesheim, R. P. Meadows, J. E. Harlan, M. Eberstadt, H. S. Yoon, S. B. Shuker, B. S. Chang, A. J. Minn, C. B. Thompson, S. W. Fesik, *Science* **1997**, *275*, 983.
- [12] M. Rosay, L. Tometich, S. Pawsey, R. Bader, R. Schauwecker, M. Blank, P. M. Borchard, S. R. Cauffman, K. L. Felch, R. T. Weber, R. J. Temkin, R. G. Griffin, W. E. Maas, *Phys. Chem. Chem. Phys.* **2010**, *12*, 5850.
- [13] Y. Hovav, A. Feintuch, S. Vega, *J. Chem. Phys.* **2011**, *134*, 074509.
- [14] D. Mance, P. Gast, M. Huber, M. Baldus, K. L. Ivanov, *J. Chem. Phys.* **2015**, *142*, 234201.
- [15] Y. Wang, O. Jardetzky, *Protein Sci.* **2002**, *11*, 852.

Received: April 6, 2016

Published online: June 28, 2016